MATERIALS SCIENCE

Self-standing and flexible covalent organic framework (COF) membranes for molecular separation

Jiangtao Liu[1,2]*, Gang Han[3]*, Dieling Zhao[1], Kangjia Lu[1], Jie Gao[1], Tai-Shung Chung[1]*†

Almost all covalent organic framework (COF) materials conventionally fabricated by solvothermal method at high temperatures and pressures are insoluble and unprocessable powders, which severely hinder their widespread applications. This work develops an effective and facile strategy to construct flexible and free-standing pure COF membranes via the liquid-liquid interface-confined reaction at room temperature and atmospheric pressure. The aperture size and channel chemistry of COF membranes can be rationally designed by bridging various molecular building blocks via strong covalent bonds. Benefiting from the highly-ordered honeycomb lattice, high solvent permeances are successfully obtained and follow the trend of acetonitrile > acetone > methanol > ethanol > isopropanol. Interestingly, the imine-linked COF membrane shows higher nonpolar solvent permeances than β-ketoenamine-linked COF due to their difference in pore polarity. Both kinds of COF membranes exhibit high solvent permeances, precise molecular sieving, excellent shape selectivity, and sufficient flexibility for membrane-based separation science and technology.

INTRODUCTION

Inspired by nature, which has created complex systems with advanced functions via atomic-level assembly, research scientists have also made great progress in constructing numerous chemical architectures from discrete [zero-dimensional (0D)] to extended structures (1D, 2D, and 3D) by assembling diverse building blocks in well-defined approaches (*1*–*3*). The superb assembling technology from building units to sophisticated architectures can be implemented via various connecting strategies based on weak interactions (π-π stacking, hydrogen bonding, or coordinate covalent bonding) or strong covalent bonding. The first family of porous nanomaterials, metal-organic frameworks (MOFs) and zeolitic imidazolate frameworks (ZIFs), could be obtained via the coordinative bonds between metal ions and organic ligands (*3*–*6*). Another family member, covalent organic frameworks (COFs), representing an exciting new type of porous organic nanomaterials with well-defined topology, honeycomb lattice, and tunable pore size, can be ingeniously constructed via strong covalent bonds of lightweight elements (C, N, O, B, etc.) (*7*–*10*). Comparing to the traditional porous nanomaterials (MOFs and ZIFs), COFs have the desirable features of totally organic metal-free backbone, low mass density, well-defined topology, permanent porosity, structural diversity, and excellent thermal resistance (*11*). The strong covalent bonds render COFs with outstanding stability in both aqueous and organic solvents. As a result, COFs have gained noteworthy attention for potential applications in gas adsorption and separation (*12*, *13*), energy storage and conversion (*14*, *15*), drug delivery (*16*, *17*), optoelectronics (*18*), sensing (*19*), and catalysis for CO_2 reduction or H_2 generation (*20*, *21*).

Since the seminal work of Yaghi and co-workers (*7*), COFs with different ordered honeycombs have sprung up in organic chemistry and materials science by introducing diverse building blocks into the frameworks. However, almost all COFs fabricated by the conventional solvothermal method under harsh reaction conditions (i.e., high temperature and pressure, inert gas protection, sealed environment, indispensable solvent, and catalyst) are insoluble and unprocessable powders, which severely hinder their applications in membrane-based separation science and technology. COFs cannot be limited to powders but have to be extended to continuous and flexible films. Development of COF-based membranes with a periodic honeycomb lattice could be a promising solution for a wide variety of separations such as water purification, valuable drug purification from organic solvents in pharma industries, oil extraction and purification in food industry, and other challenging separations. As time goes by, both bottom-up (i.e., in situ growth on surface, vapor-assisted conversion, and layer-by-layer stacking) and top-down (i.e., solvent-assisted exfoliation, chemical exfoliation, mechanical delamination, and blending) synthetic strategies have been explored for the fabrication of COF membranes (*22*–*26*). Unfortunately, neither of them can accomplish the goal of preparing free-standing and pure COF membranes with good flexibility at a large scale.

Interfacial polymerization (IP) currently dominates the fabrication of commercial reverse osmosis and nanofiltration membranes due to its scalability and feasibility (*27*–*29*). The concept of interface-confined reaction can be explored for the synthesis of COF films. The fabrication of COF membranes at the liquid-liquid interface was reported in 2017 (*30*). In that study, the amine monomers were dissolved in the aqueous phase. However, most of the aromatic amine monomers had poor solubility in water, and the resultant COF films had relatively low mechanical strength and needed to be sandwiched between two polyester supports for filtration tests. More recently, the Lewis acid $Sc(OTf)_3$ was used as the catalyst for COF membrane syntheses (*31*). However, an expensive and environment-unfriendly metal-triflate catalyst was involved, which would be undesirable for large-scale practical applications. IP at the liquid-air interface was also explored for the preparation of COF membranes (*32*–*35*). Transferring this COF thin layer from the water surface onto the support was conducted by a Langmuir-Blodgett method. This process usually needed to be repeated many times to get a robust nanofiltration membrane, and the amine monomers must be amphiphilic to interpose between toluene and water phases. It is still a

[1]Department of Chemical and Biomolecular Engineering, National University of Singapore, Singapore 117585, Singapore. [2]Ningbo Institute of Material Technology and Engineering, Chinese Academy of Sciences, Ningbo 315201, China. [3]Department of Chemical Engineering, Massachusetts Institute of Technology, Cambridge, MA 02139, USA.
*These authors contributed equally to this work.
†Corresponding author. Email: chencts@nus.edu.sg

monumental challenge to fabricate continuous free-standing COF films in large scale via IP process.

In this work, we have successfully developed an effective and simple method to fabricate continuous self-standing COF nanofilms at room temperature and atmospheric pressure via an innovative interface–confined reaction. Undoubtedly, this simple and mild strategy surpasses the traditional solvothermal method, which is notorious for high-energy consumption, complex operations, and possible release of volatile organic compounds. These COF films have good flexibility, which can be transferred onto any substrate without damaging their structure. Even after drying, the self-standing COF thin films can still maintain their flexibility and integrity. To the best of our knowledge, this is the leading report that demonstrates the fabrication of self-standing and flexible pure COF membranes at a large scale via interface-confined reaction at room temperature and atmospheric pressure. Furthermore, these defect-free COF thin films have been successfully evaluated for molecular sieving separations with an ultrafast solvent permeance and excellent shape selectivity.

RESULTS

Construction and characterizations of the self-standing COF thin films

As indicated in Fig. 1, an ingenious approach was developed to fabricate self-standing COF films with well-defined pore channels by confining the polymerization of aldehyde and amine monomers at the interface between dichloromethane (DCM) and water. Figure 1 shows the optimal IP procedure for COF nanofilm fabrication, while fig. S1 shows COF films constructed by nanospheres. COF films fabricated from Fig. 1 are flexible and defect free for molecular separation in nanofiltration tests; however, COF films from fig. S1 are brittle, defective, and have no rejection for dye molecules. As the IP procedure shown in fig. S1, the tris(4-aminophenyl)amine (TAPA) and catalyst aqueous phase was added directly onto the organic phase [2,4,6-triformylphloroglucinol (TFP) in DCM], and then the interfacial reaction started immediately and vigorously after the two phases contacted. The interface between the organic and aqueous phase was unstable under flow when adding the TAPA/catalyst aqueous phase. Thus, the resultant COF film was not smooth and uniform but full of nanoparticles/nanospheres, as shown in fig. S1 [scanning electron microscopy (SEM) images]. We attribute these nanoparticles/nanospheres to the presence of aqueous emulsion droplets near the unstable interface after the addition of the aqueous phase. Furthermore, the COF nanoparticle size can be tuned by the catalyst amount. When 1.8 mmol of acetic acid was used, the COF nanoparticle size was about 1 μm after 24-hour interfacial reaction. When the acetic acid amount increased to 3.6 mmol, the nanoparticle size decreased to 100 nm. These COF nanoparticles are uniform but undesirable for separation since the COF membranes from fig. S1 are brittle and have no rejections for dye molecules. Different from the IP procedure in fig. S1, Fig. 1 illustrates that both aldehyde and amine monomers were dissolved in the organic phase (TFP/TAPA in DCM), while the catalyst was then gently added into the water phase. This pure water layer was critical for the synthesis of flexible and defect-free COF films, and it allowed slow diffusion of the acetic acid to the interface and prevented unstable interface and vigorous interfacial reaction, leading to the formation of continuous and homogeneous COF films at room temperature. Here, the thicknesses of COF membranes were time dependent and could be regulated from as low as 5 nm to as high as 300 nm, depending on the interfacial reaction time from 1 min to 24 hours, as shown in fig. S2. If the flexible and defect-free COF films were treated in *N*,*N*′-dimethylformamide for 30 days, then the highly ordered microstructure appeared, and the top surface and bottom surface were sharply different, as shown in fig. S3 (SEM images). The cross sections were full of nanocolumns, and the bottom surface was rough, while the top surface was still smooth, uniform, and dense. Consequently, the rejection ratio for dye molecules was high, while the COF films constructed by nanospheres had no rejection in nanofiltration tests. Therefore, membrane-based separation technologies prefer the flexible and defect-free COF films constructed by nanocolumns but not the films constructed by nanospheres (*36*). In general, perfect COF single-crystal powders are beautiful but not so useful in practical separation applications (*37*). Figure 1 shows the chemical structures of TAPA-TFP and TAPA-TFB (1,3,5-triformylbenzene, TFB) COF films from the optimal IP procedure. Because of the self-sealing and self-termination features of IP, the resultant self-standing COF films were only 300 nm in thickness, but they had sufficient mechanical strength and could easily be taken out from water and transferred to the substrates (fig. S6). As shown in movie S1 (TAPA-TFP) and movie S2 (TAPA-TFB), no visible tear and fragmentation occurred after several successive violent pulls and rips. Even after drying, the self-standing COF films could still maintain their flexibility and integrity, which strongly verifies their mechanical robustness (movie S3).

To gain insight into the internal structure, we transferred these self-standing COF thin films to anodized aluminum oxide (AAO) substrates and silicon wafers, where field-emission SEM (FESEM) and atomic force microscopy (AFM) were used to confirm their thickness, surface morphology, and cross section, as shown in Fig. 2. Thicknesses of these self-standing COF thin films were about 300 nm and quite uniform, evaluated from the cross-sectional FESEM images. In addition, height analyses measured by AFM from the silicon wafer to the film surface also confirmed the thickness of 300 nm. The thinnest COF layer fabricated in this work was about 5 nm, as shown in fig. S2, which was about 10 single COF layers stacking together. Because of the self-sealing and self-termination features of IP, the COF film almost reached the maximum thickness after 24 hours. During the interfacial reaction, the region between DCM and water interface was within a molecule-level thickness; therefore, in this confined space, the molecule building blocks were forced to generate a 2D COF layer with an atomic thickness. Layer-by-layer growth of the thin COF layer at the confined interface was the main mechanism to form self-standing COF films with good mechanical robustness. Therefore, it is easy to manipulate the COF films with thicknesses ranging from several to hundreds of nanometer by controlling the reaction duration and the monomer concentration. A further close inspection from 3D AFM images disclosed the surface morphology, and the average roughness (Ra) of both TAPA-TFP and TAPA-TFB films were lower than 3 nm, indicating an extremely smooth surface. As a result, the self-standing COF thin films floating in water showed a mirror-like shiny surface (movie S1).

The chemical structures of COF films were characterized by Fourier transform infrared spectroscopy and x-ray photoelectron spectroscopy (XPS) analyses. As depicted in fig. S4, the disappearance of amine N—H stretching bands at 3200 cm^{-1} with the appearance of a new C═N stretching peak at 1250 cm^{-1} and a C═C stretching peak at 1560 cm^{-1} indicates the successful formation of Schiff-base structure in the resultant COF films. In addition, the shift of C═O stretching peak from 1658 to 1615 cm^{-1} confirms the presence of β-ketoenamine

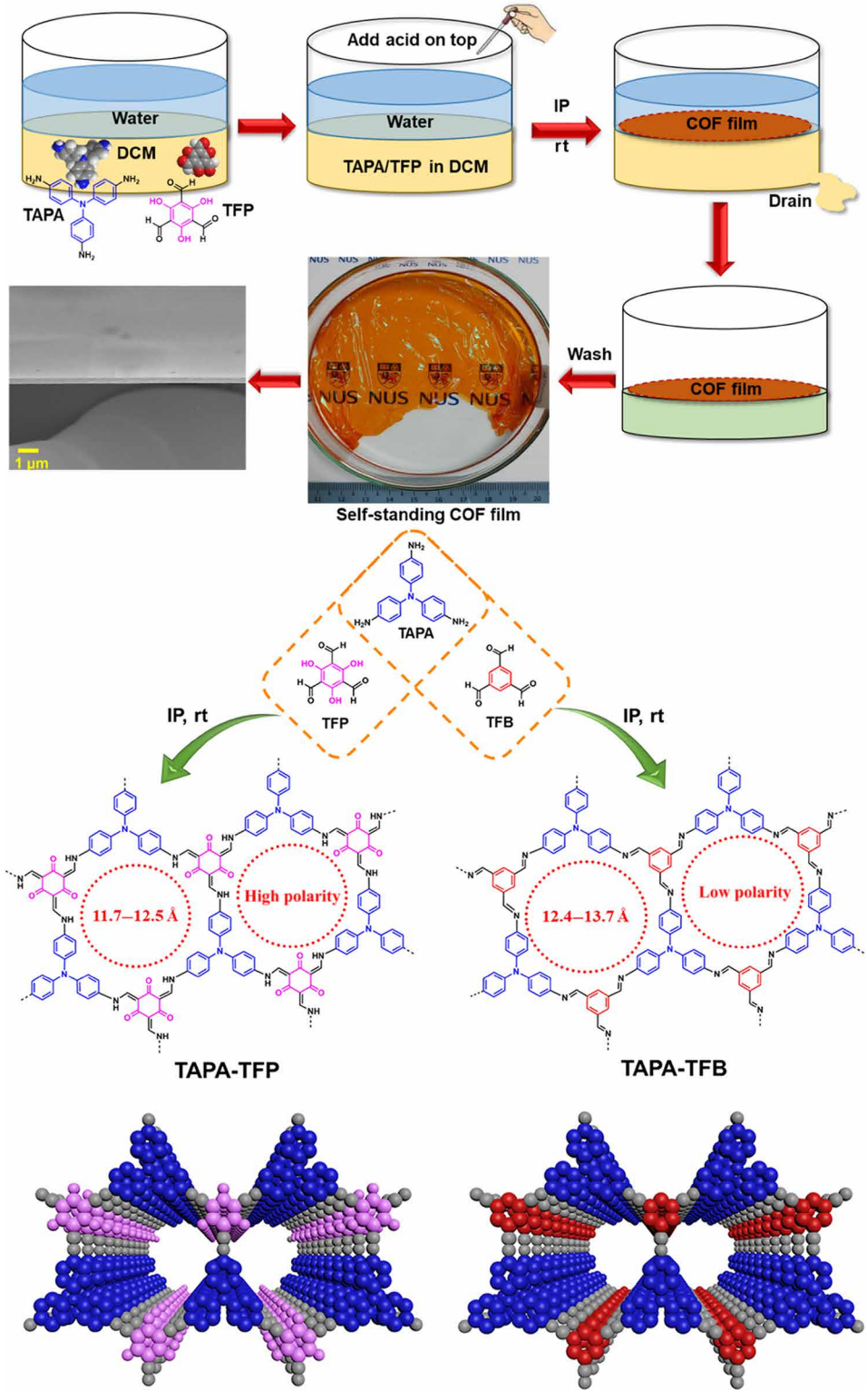

Fig. 1. Fabrication process and chemical structures of the self-standing COF films. (Photo credit: Jiangtao Liu, National University of Singapore). IP, interfacial polymerization; rt, room temperature.

linkages in the resultant TAPA-TFP framework. In general, the characteristic peaks of —CHO and —NH_2 groups of the precursors disappear in the final COF thin films, which indicates a complete conversion of the starting aldehyde and amine monomers. XPS analyses in fig. S4 provide additional evidence for the formation of imine bonds. The C 1s spectrum at 281.4 eV can be assigned to the C backbone. At the same time, the N 1s spectrum at 396.5 eV can be attributed to the N in imine bonds. The sharp difference between TAPA-TFP

and TAPA-TFB is the O 1s peak, where the O 1s peak is clearly observed in the TAPA-TFP film but is almost not found in TAPA-TFB, which is consistent with their chemistry. Table S1 summarizes the atomic compositions obtained from the XPS spectra, and all the elements in TAPA-TFP and TAPA-TFB frameworks match well with their theoretical values, which strongly confirm the proposed structures shown in Fig. 1.

X-ray diffraction (XRD) was performed to gain insights into the highly ordered structure of these COF films. As shown in fig. S5, the experimental results agree well with the simulated XRD patterns. The TAPA-TFP film shows a sharp and intense peak at a lower 2θ value of 6.5°, which is assigned to the reflection of the (100) plane with a pore aperture of about 13.6 Å. The (100) plane peak of the TAPA-TFB thin film shifts to a little higher 2θ value of 6.7°, indicating its slightly smaller pore aperture of 13.2 Å. The pore sizes evaluated from XRD results match well with the predicated aperture sizes of TAPA-TFP (11.7 to 12.5 Å) and TAPA-TFB (12.4 to 13.7 Å) films shown in Fig. 1. The last broad peak at the highest 2θ angle of 22.4° is attributed to the (001) plane caused by π-π stacking between the highly ordered successive COF layers. However, a substantial difference in the relative intensity of the XRD peaks was observed in this two COF films. For example, the peak at 6.7° has a relatively stronger intensity than the peak at 22.4° for the TAPA-TFP film, while the TAPA-TFB film shows an opposite trend, indicating the higher crystalline structure of the former. Usually, the β-ketoenamine–linked TAPA-TFP COF is considerably more crystalline and stable than imine-linked TAPA-TFB due to more hydrogen bonds in TAPA-TFP (*38*–*40*). The gaps between the successive COF layers are found to be 3.9 Å, estimated from the π-π stacking XRD peak at 22.4°, which is consistent with the eclipsed stacking model in Fig. 1.

Superhighways for rapid polar and nonpolar solvent transport

Figure 3A shows the permeances of pure polar and nonpolar solvents through COF membranes. As summarized in table S2, benefiting from the highly ordered honeycomb lattice, extremely high permeances through the TAPA-TFP thin film are achieved following the order of acetonitrile (381.6 liters m^{-2} $hour^{-1}$ bar^{-1}) > acetone (324.5 liters m^{-2} $hour^{-1}$ bar^{-1}) > methanol (241.9 liters m^{-2} $hour^{-1}$ bar^{-1}) > ethanol (127.3 liters m^{-2} $hour^{-1}$ bar^{-1}) > isopropanol (25.4 liters m^{-2} $hour^{-1}$ bar^{-1}) > dimethylformamide (8.1 liters m^{-2} $hour^{-1}$ bar^{-1}), which is exactly on the opposite order of their kinetic diameters and viscosity. The TAPA-TFB membrane has a similar order of solvent transport but slightly lower permeances. The TAPA-TFP film (11.7 to 12.5 Å) has a relative smaller pore size than the TAPA-TFB film (12.4 to 13.7 Å), but the former has higher permeances of polar organic solvents than the latter. The TAPA-TFP has relatively hydrophilic channels with polar N—H and C═O covalent bonds on its pore wall. As a result, it has higher and favorable affinity toward polar solvents. In contrast, the TAPA-TFB membrane has a larger pore window but relatively hydrophobic channels. Thus, it has higher permeances to nonpolar solvents such as cyclohexane (53.4 liters m^{-2} $hour^{-1}$ bar^{-1}) and n-hexane (109.8 liters m^{-2} $hour^{-1}$ bar^{-1}), which are almost five times higher than those of the TAPA-TFP membrane.

Usually, the solvent permeances through COF membranes are governed by the aperture size, solvent viscosity, and polarity, as well as solvent-membrane interactions. In general, the larger the aperture size and the lower the solvent viscosity, the higher is the permeance. Considering the TAPA-TFP and TAPA-TFB COF thin films with comparable pore sizes, the TAPA-TFP film with high polar channels exhibits higher fluxes for polar organic solvents than the TAPA-TFB film with low polar channels. Note that the TAPA-TFP film has a methanol flux of 241.9 liters m^{-2} $hour^{-1}$ bar^{-1}, near 4 times higher than the existing polyamide-based nanofiltration membrane (52.2 liters m^{-2} $hour^{-1}$ bar^{-1}) and about 500 times higher than the commercially available organic solvent nanofiltration membrane, DuraMem DM150 (0.48 liters m^{-2} $hour^{-1}$ bar^{-1}) (*28*). The ultrafast solvent permeance and high solute separation performance are clearly demonstrated in the benchmarking table S3. Therefore, the ultrafast flux can be ascribed to their intrinsic microporosity that has permanent superhighways for rapid solvent transport (*41*–*43*). In contrast, the conventional polyamide-based membranes with extrinsic microporosity have twisted and tortuous pore channels, which increase the solvent transport path and resistance. The ultrafast polar and nonpolar organic solvent permeances may pave the way for the self-standing COF films in purification of valuable chemicals and recovery of solvents from pharmaceutical and petrochemical industries with great energy efficiency.

Precise molecular sieving effects

The increasing contamination of organic micropollutants in environmental and biological systems is one of the serious issues faced by humanity. The potentially harmful effects of organic micropollutants (pesticides, pharmaceuticals, and dyes) on human health and aquatic ecosystems have raised worldwide concerns. The releasing of organic micropollutants to fresh water causes serious health hazards because most of them are mutagenic or carcinogenic in nature (*44*). Until now, porous-activated carbons and polymers have been widely used as adsorbents for the removal of organic micropollutants from wastewater. However, these materials have fatal drawbacks, (i) regeneration of spent activated carbons are energy intensive (heating to 500° to 900°C), (ii) regeneration of porous polymers needs soaking the spent adsorbents in extraction solvents for desorption, and (iii) their performance often declines after several recycles (*45*). Comparing with absorbents, membrane technology has merits of high separation performance, low energy consumption, mild operation temperature, cost efficiency, and no cross contamination, etc. Therefore, it has a great environmental and industrial significance to evaluate the molecular sieving effect of COF films for the removal of organic contaminants. Here, dyes with different molecular weights and dimensions were chosen as the models of organic micropollutants. As shown in Fig. 3B, the self-standing COF films with a periodic honeycomb lattice show high rejections to dyes with molecular sizes larger than the COF aperture sizes. Both COF films can almost fully reject Alcian blue (AB; 24.5 × 26.1 Å), brilliant blue R (BBR; 17.9 × 20.6 Å), and vitamin B12 (14.2 × 18.3 Å) but only partially reject rose bengal (RB; 11.2 × 12.4 Å). The TAPA-TFP shows relatively higher rejections than the TAPA-TFB due to its smaller aperture size. The long-term nanofiltration tests and ultraviolet spectra of various dyes before and after filtration through TAPA-TFP COF membranes are shown in fig. S7.

In general, the rejection is determined by a very complex interplay among solute size, solvent viscosity, solute-solvent interaction, and aperture size of the membrane. In aquatic solutions, the charge interactions between the solute and membrane surface play an important role in rejection. However, the charge effects may become very weak in organic solvents since the ionic dyes are difficult to dissociate. As a result, the membrane rejection is mainly determined by the molecular sieving effect and shape-selective function. The

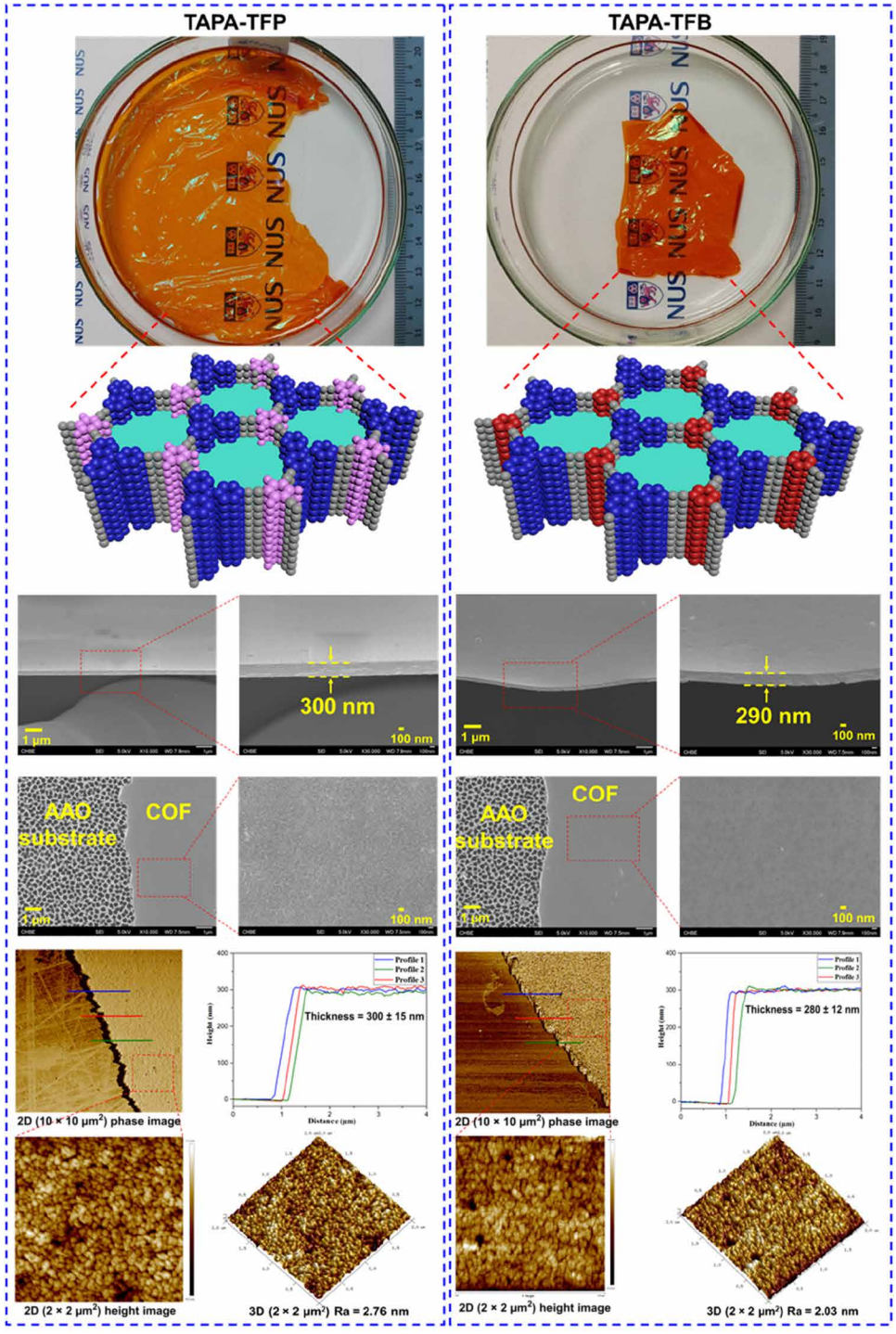

Fig. 2. Thickness and surface morphology of the self-standing COF films evaluated from FESEM and AFM. (Photo credit: Jiangtao Liu, National University of Singapore).

effective molecular size of a dye molecule depends on the short-end kinetic diameter of its 3D bulky structure, as illustrated in Fig. 4. For instance, the long-end kinetic diameter of RB is around 12.4 Å, while its short-end kinetic diameter is around 11.2 Å. On the basis of the aperture sizes of TAPA-TFP (11.7 to 12.5 Å) and TAPA-TFB (12.4 to 13.7 Å), RB with a small effective molecular size of 11.2 Å can easily pass through these channels, while AB and BBR with lager effective molecular sizes are almost completely blocked. According to the relationship between rejections and molecular dimensions, the estimated cutoff molecular size is about 13 Å, which is very close to the aperture sizes of these COFs.

DISCUSSION

Molecular sieving processes, for gas, ions, or molecules, often suffer from (i) trade-off relations between permeability (or permeance)

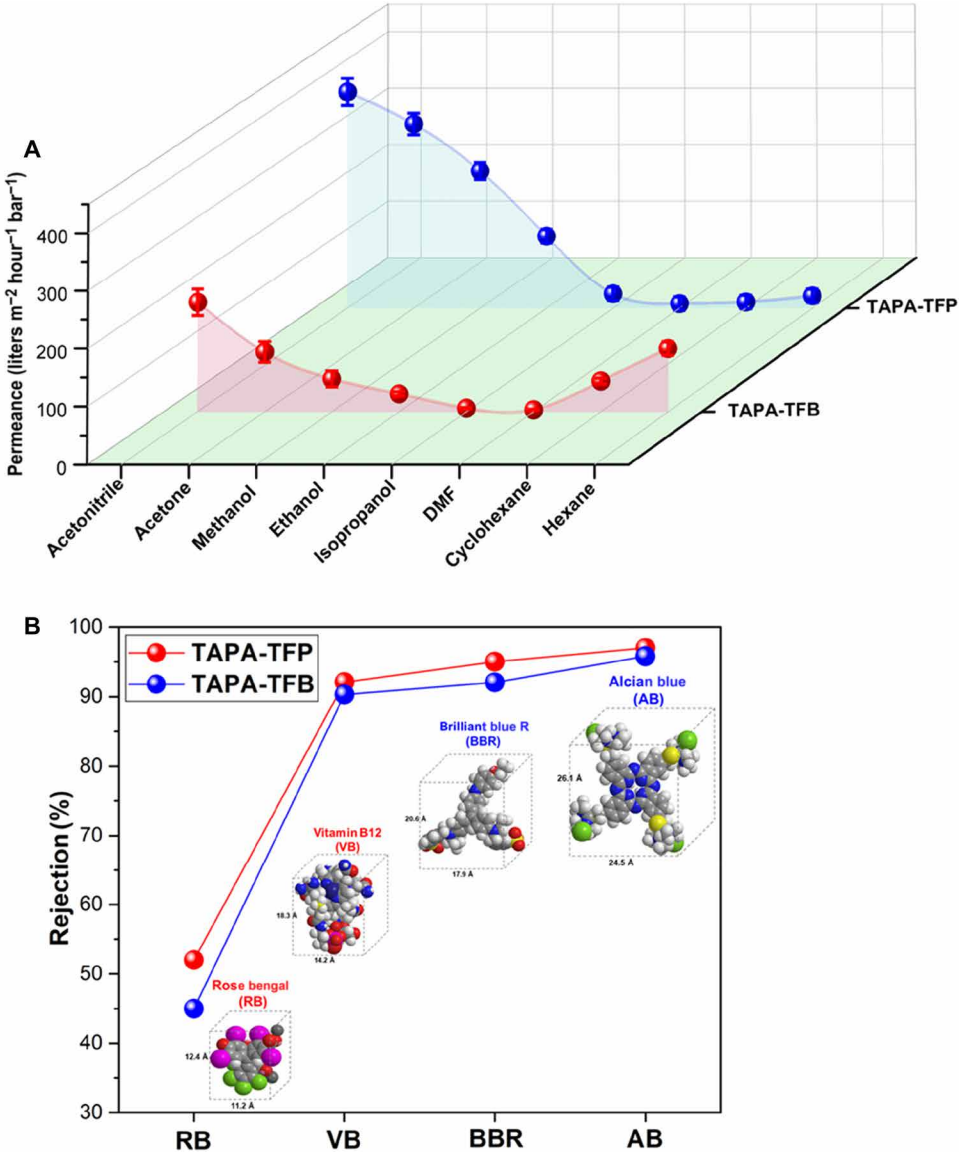

Fig. 3. Permeation and rejection performance of the COF membranes. (**A**) The polar and nonpolar solvent permeances. (**B**) The rejection of COF membranes toward dyes with different molecular sizes in ethanol.

and selectivity (or rejection), (ii) poor chemical and thermal stabilities in practical applications, and (iii) high cost and energy consumption in fabrication, which are the Achilles heels of membrane separation science and technology. The unique merits of flexible COF membranes, such as (i) highly ordered honeycomb lattice and tunable pore size at molecular level, (ii) strong covalent bond–bridged building blocks, and (iii) interfacial fabrication at room temperature and atmospheric pressure, not only endow traditional COF nanomaterials with new fascination but also open up new perspectives for membrane-based separation science and technology. Different from COF powders synthesized by the conventional solvothermal method under harsh conditions (i.e., high temperature and pressure, inert gas protection, sealed environment, indispensable solvents, and catalysts), in this work, the continuous self-standing and flexible COF membranes have been successfully constructed via an innovative interface–confined reaction between the aldehyde and amine molecular building blocks at room temperature and atmospheric pressure. The high-polar inner cavities of TAPA-TFP provide superhighways for polar solvent molecules, while the low-polar inner cavities of TAPA-TFB facilitate the transport of nonpolar solvents. The methanol permeance (241.9 liters m^{-2} hour^{-1} bar^{-1}) of TAPA-TFP was about four times higher than the existing polyamide-based nanofiltration membrane. The high solute (>13 Å) separation performance was mainly based on the molecular sieving effect and the shape-selective function. Comparing to MOFs and ZIFs, COFs have the desirable features of totally organic metal-free backbone, lower mass density, and higher water stability, which are highly desired in various membrane-based separation technologies. We believe that the continuous COF membranes with superhighways for solvent transport and shape-selective functions for molecular sieving, coupled with good mechanical flexibility and fabrication simplicity, have great potential applications for (i) the removal of organic micropollutants

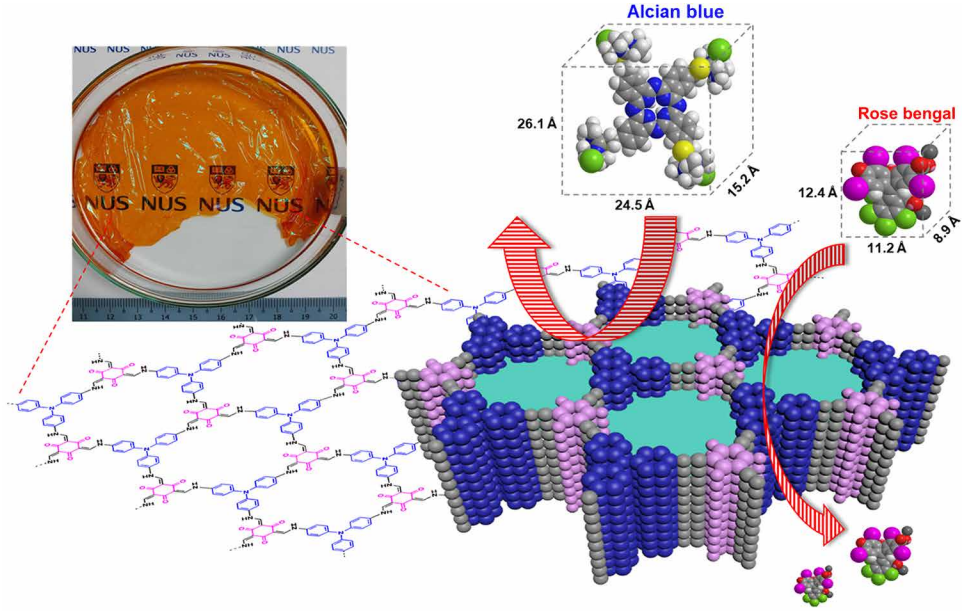

Fig. 4. The schematic diagram of molecular transport through the COF membrane. (Photo credit: Jiangtao Liu, National University of Singapore).

from environmental and biological systems, (ii) drug purification in the pharmaceutical industry, (iii) oil extraction and purification in the food industry, and (iv) other challenging separations (i.e., hemodialysis or chiral separation). Meanwhile, roadblocks may still exist on the way to shift the interfacial fabrication technology from flat-sheet membranes to hollow fibers, and the growing mechanisms of COF layer in the confined-interface reaction still need further clarification. Therefore, we acknowledge that more research work from the basic reaction mechanisms to the real industrial implements would have to be performed by the successor.

MATERIALS AND METHODS

Fabrication of the self-standing COF films

The self-standing and flexible COF nanofilms were fabricated via interfacial reaction between aldehyde and amine building blocks at room temperature and atmospheric pressure. Before the optimized IP procedure was used, as illustrated in fig. S1, different procedures were explored. The optimal synthesis procedure was carried out as follows: TAPA (174.3 mg, 0.6 mmol) and TFP (126.1 mg, 0.6 mmol) or TFB (97.3 mg, 0.6 mmol) were dissolved in 100 ml of DCM as the organic phase. As illustrated in Fig. 1, the TAPA and TFP solutions were poured into a glass petri dish together as the organic phase, and then pure water was slowly added onto the top surface of the DCM solution, leaving a stable DCM/water interface. Subsequently, 1.2 ml of aqueous acetic acid (3.0 M) was gently added into the aqueous phase as the catalyst. Afterward, the petri dish was covered to keep it under a stable condition and avoid airflow. A transparent and smooth thin film was clearly observed at the interface between the two immiscible phases. After interfacial reaction at room temperature for 24 hours, both the aqueous and organic solutions were drained off, leaving the resultant free-standing thin film in the petri dish. The free-standing thin film was rinsed several times by deionized water and acetone to wash away the residual monomers and then transferred to an AAO membrane substrate or preserved in ultrapure water for further characterizations.

SUPPLEMENTARY MATERIALS

Supplementary material for this article is available at http://advances.sciencemag.org/cgi/content/full/6/41/eabb1110/DC1

REFERENCES AND NOTES

1. C. S. Diercks, O. M. Yaghi, The atom, the molecule, and the covalent organic framework. *Science* **355**, eaal1585 (2017).
2. J. W. Colson, W. R. Dichtel, Rationally synthesized two-dimensional polymers. *Nat. Chem.* **5**, 453–465 (2013).
3. H. Li, M. Eddaoudi, M. O'Keeffe, O. M. Yaghi, Design and synthesis of an exceptionally stable and highly porous metal-organic framework. *Nature* **402**, 276–279 (1999).
4. H. Hayashi, A. P. Cote, H. Furukawa, M. O'Keeffe, O. M. Yaghi, Zeolite a imidazolate frameworks. *Nat. Mater.* **6**, 501–506 (2007).
5. H. Furukawa, K. E. Cordova, M. O'Keeffe, O. M. Yaghi, The chemistry and applications of metal-organic frameworks. *Science* **341**, 1230444 (2013).
6. B. M. Weckhuysen, J. Yu, Recent advances in zeolite chemistry and catalysis. *Chem. Soc. Rev.* **44**, 7022–7024 (2015).
7. A. P. Cote, A. I. Benin, N. W. Ockwig, M. O'keeffe, A. J. Matzger, O. M. Yaghi, Porous, crystalline, covalent organic frameworks. *Science* **310**, 1166–1170 (2005).
8. N. Huang, P. Wang, D. Jiang, Covalent organic frameworks: A materials platform for structural and functional designs. *Nat. Rev. Mater.* **1**, 16068 (2016).
9. E. Q. Jin, M. Asada, Q. Xu, S. Dalapati, M. A. Addicoat, M. A. Brady, H. Xu, T. Nakamura, T. Heine, Q. H. Chen, D. Jiang, Two-dimensional sp^2 carbon-conjugated covalent organic frameworks. *Science* **357**, 673–676 (2017).
10. E. L. Spitler, W. R. Dichtel, Lewis acid-catalysed formation of two-dimensional phthalocyanine covalent organic frameworks. *Nat. Chem.* **2**, 672–677 (2010).
11. Y. Song, Q. Sun, B. Aguila, S. Ma, Opportunities of covalent organic frameworks for advanced applications. *Adv. Sci.* **6**, 1801410 (2019).
12. F. Hiroyasu, O. M. Yaghi, Storage of hydrogen, methane, and carbon dioxide in highly porous covalent organic frameworks for clean energy applications. *J. Am. Chem. Soc.* **131**, 8875–8883 (2009).
13. N. Huang, X. Chen, R. Krishna, D. Jiang, Two-dimensional covalent organic frameworks for carbon dioxide capture through channel-wall functionalization. *Angew. Chem. Int. Ed.* **54**, 2986–2990 (2015).
14. F. Xu, H. Xu, X. Chen, D. Wu, Y. Wu, H. Liu, C. Gu, R. Fu, D. Jiang, Radical covalent organic frameworks: A general strategy to immobilize open-accessible polyradicals for high-performance capacitive energy storage. *Angew. Chem. Int. Ed.* **54**, 6814–6818 (2015).
15. C. R. DeBlase, K. E. Silberstein, T. T. Truong, H. D. Abruña, W. R. Dichtel, β-Ketoenamine-linked covalent organic frameworks capable of pseudocapacitive energy storage. *J. Am. Chem. Soc.* **135**, 16821–16824 (2013).
16. Q. Fang, J. Wang, S. Gu, R. B. Kaspar, Z. Zhuang, J. Zheng, H. Guo, S. Qiu, Y. Yan, 3D porous crystalline polyimide covalent organic frameworks for drug delivery. *J. Am. Chem. Soc.* **137**, 8352–8355 (2015).

17. L. Bai, S. Z. F. Phua, W. Q. Lim, A. Jana, Z. Luo, H. P. Tham, L. Zhao, Q. Gao, Y. Zhao, Nanoscale covalent organic frameworks as smart carriers for drug delivery. *Chem. Commun.* **52**, 4128–4131 (2016).
18. N. Keller, D. Bessinger, S. Reuter, M. Calik, L. Ascherl, F. C. Hanusch, F. Auras, T. Bein, Oligothiophene-bridged conjugated covalent organic frameworks. *J. Am. Chem. Soc.* **139**, 8194–8199 (2017).
19. S. Dalapati, S. B. Jin, J. Gao, Y. H. Xu, A. Nagai, D. L. Jiang, An azine-linked covalent organic framework. *J. Am. Chem. Soc.* **135**, 17310–17313 (2013).
20. S. Lin, C. S. Diercks, Y.-B. Zhang, N. Kornienko, E. M. Nichols, Y. Zhao, A. R. Paris, D. Kim, P. Yang, O. M. Yaghi, C. J. Chang, Covalent organic frameworks comprising cobalt porphyrins for catalytic CO_2 reduction in water. *Science* **349**, 1208–1213 (2015).
21. V. S. Vyas, F. Haase, L. Stegbauer, G. Savasci, F. Podjaski, C. Ochsenfeld, B. V. Lotsch, A tunable azine covalent organic framework platform for visible light-induced hydrogen generation. *Nat. Commun.* **6**, 8508 (2015).
22. J. W. Colson, A. R. Woll, A. Mukherjee, M. P. Levendorf, E. L. Spitler, V. B. Shields, M. G. Spencer, J. Park, W. R. Dichtel, Oriented 2D covalent organic framework thin films on single-layer graphene. *Science* **332**, 228–231 (2011).
23. S. Yuan, X. Li, J. Zhu, G. Zhang, P. Van Puyvelde, B. Van Der Bruggen, Covalent organic frameworks for membrane separation. *Chem. Soc. Rev.* **48**, 2665–2681 (2019).
24. X.-H. Liu, C.-Z. Guan, S.-Y. Ding, W. Wang, H.-J. Yan, D. Wang, L.-J. Wan, On-surface synthesis of single-layered two-dimensional covalent organic frameworks via solid-vapor interface reactions. *J. Am. Chem. Soc.* **135**, 10470–10474 (2013).
25. H. Fan, J. Gu, H. Meng, A. Knebel, J. Caro, High-flux membranes based on the covalent organic framework COF-LZU1 for selective dye separation by nanofiltration. *Angew. Chem. Int. Ed.* **57**, 4083–4087 (2018).
26. S. Kandambeth, B. P. Biswal, H. D. Chaudhari, K. C. Rout, H. Shebeeb Kunjattu, S. Mitra, S. Karak, A. Das, R. Mukherjee, U. K. Kharul, R. Banerjee, Selective molecular sieving in self-standing porous covalent-organic-framework membranes. *Adv. Mater.* **29**, 1603945 (2017).
27. P. Marchetti, M. F. Jimenez Solomon, G. Szekely, A. G. Livingston, Molecular separation with organic solvent nanofiltration: A critical review. *Chem. Rev.* **114**, 10735–10806 (2014).
28. S. Karan, Z. Jiang, A. G. Livingston, Sub-10 nm polyamide nanofilms with ultrafast solvent transport for molecular separation. *Science* **348**, 1347–1351 (2015).
29. J. T. Liu, D. Hua, Y. Zhang, S. Japip, T. S. Chung, Precise molecular sieving architectures with Janus pathways for both polar and nonpolar molecules. *Adv. Mater.* **30**, 1705933 (2018).
30. K. Dey, M. Pal, K. C. Rout, H. Shebeeb Kunjattu, A. Das, R. Mukherjee, U. K. Kharul, R. Banerjee, Selective molecular separation by interfacially crystallized covalent organic framework thin films. *J. Am. Chem. Soc.* **139**, 13083–13091 (2017).
31. M. Matsumoto, L. Valentino, G. M. Stiehl, H. B. Balch, A. R. Corcos, F. Wang, D. C. Ralph, B. J. Mariñas, W. R. Dichtel, Lewis-acid-catalyzed interfacial polymerization of covalent organic framework films. *Chem* **4**, 308–317 (2018).
32. D. B. Shinde, G. Sheng, X. Li, M. Ostwal, A.-H. Emwas, K.-W. Huang, Z. Lai, Crystalline 2D covalent organic framework membranes for high-flux organic solvent nanofiltration. *J. Am. Chem. Soc.* **140**, 14342–14349 (2018).
33. J. I. Feldblyum, C. H. McCreery, S. C. Andrews, T. Kurosawa, E. J. G. Santos, V. Duong, L. Fang, A. L. Ayzner, Z. N. Bao, Few-layer, large-area, 2D covalent organic framework semiconductor thin films. *Chem. Commun.* **51**, 13894–13897 (2015).
34. W. Dai, F. Shao, J. Szczerbiński, R. McCaffrey, R. Zenobi, Y. Jin, A. D. Schlüter, W. Zhang, Synthesis of a two-dimensional covalent organic monolayer through dynamic imine chemistry at the air/water interface. *Angew. Chem. Int. Ed.* **55**, 213–217 (2016).
35. H. Sahabudeen, H. Qi, B. A. Glatz, D. Tranca, R. Dong, Y. Hou, T. Zhang, C. Kuttner, T. Lehnert, G. Seifert, U. Kaiser, A. Fery, Z. Zheng, X. Feng, Wafer-sized multifunctional polyimine-based two-dimensional conjugated polymers with high mechanical stiffness. *Nat. Commun.* **7**, 13461 (2016).
36. H. S. Sasmal, A. Halder, H. Shebeeb Kunjattu, K. Dey, A. Nadol, T. G. Ajithkumar, P. R. Bedadur, R. Banerjee, Covalent self-assembly in two dimensions: Connecting covalent organic framework nanospheres into crystalline and porous thin films. *J. Am. Chem. Soc.* **141**, 20371–20379 (2019).
37. T. Ma, E. A. Kapustin, S. X. Yin, L. Liang, Z. Zhou, J. Niu, L.-H. Li, Y. Wang, J. Su, J. Li, X. Wang, W. D. Wang, W. Wang, J. Sun, O. M. Yaghi, Single-crystal x-ray diffraction structures of covalent organic frameworks. *Science* **361**, 48–52 (2018).
38. S. Kandambeth, K. Dey, R. Banerjee, Covalent organic frameworks: Chemistry beyond the structure. *J. Am. Chem. Soc.* **141**, 1807–1822 (2019).
39. A. Halder, S. Karak, M. Addicoat, S. Bera, A. Chakraborty, S. H. Kunjattu, P. Pachfule, T. Heine, R. Banerjee, Ultrastable imine-based covalent organic frameworks for sulfuric acid recovery: An effect of interlayer hydrogen bonding. *Angew. Chem. Int. Ed.* **57**, 5797–5802 (2018).
40. S. Kandambeth, A. Mallick, B. Lukose, M. V. Mane, T. Heine, R. Banerjee, Construction of crystalline 2D covalent organic frameworks with remarkable chemical (acid/base) stability via a combined reversible and irreversible route. *J. Am. Chem. Soc.* **134**, 19524–19527 (2012).
41. Y. Li, Q. X. Wu, X. H. Guo, M. C. Zhang, B. Chen, G. Y. Wei, X. Li, X. F. Li, S. J. Li, L. J. Ma, Laminated self-standing covalent organic framework membrane with uniformly distributed subnanopores for ionic and molecular sieving. *Nat. Commun.* **11**, 599 (2020).
42. R. Wang, X. Shi, A. Xiao, W. Zhou, Y. Wang, Interfacial polymerization of covalent organic frameworks (COFs) on polymeric substrates for molecular separations. *J. Membr. Sci.* **566**, 197–204 (2018).
43. M. Galizia, K. P. Bye, Advances in organic solvent nanofiltration rely on physical chemistry and polymer chemistry. *Front. Chem.* **6**, 511 (2018).
44. R. P. Schwarzenbach, B. I. Escher, K. Fenner, T. B. Hofstetter, C. A. Johnson, U. Von Gunten, B. Wehrli, The challenge of micropollutants in aquatic systems. *Science* **313**, 1072–1077 (2006).
45. A. Alsbaiee, B. J. Smith, L. Xiao, Y. Ling, D. E. Helbling, W. R. Dichtel, Rapid removal of organic micropollutants from water by a porous β-cyclodextrin polymer. *Nature* **529**, 190–194 (2016).

Acknowledgments: Thanks are given to Z. Cheng, Y. Zhang, Y. Xu, S. Japip, and C. Wan for assistance and discussion in the research process. **Funding:** We would like to thank the National Research Foundation, Prime Minister's Office, Singapore for funding this research under Competitive Research Program for the project entitled "Development of solvent resistant nanofiltration membranes for sustainable pharmaceutical and petrochemical manufacture" [CRP award no. NRF-CRP14-2014-01 (NUS grant number: R-279-000-466-281)].
Author contributions: J.L. and T.-S.C. conceived the project. J.L. performed the experiments, conducted formal data analysis, and wrote the manuscript. All authors discussed the results and commented on the manuscript. **Competing interests:** The authors declare that they have no competing interests. **Data and materials availability:** All data needed to evaluate the conclusions in the paper are present in the paper and/or the Supplementary Materials. Additional data related to this paper may be requested from the authors.

Submitted 31 January 2020
Accepted 19 August 2020
Published 7 October 2020
10.1126/sciadv.abb1110

Citation: J. Liu, G. Han, D. Zhao, K. Lu, J. Gao, T.-S. Chung, Self-standing and flexible covalent organic framework (COF) membranes for molecular separation. *Sci. Adv.* **6**, eabb1110 (2020).

Science Advances

Self-standing and flexible covalent organic framework (COF) membranes for molecular separation

Jiangtao Liu, Gang Han, Dieling Zhao, Kangjia Lu, Jie Gao and Tai-Shung Chung

Sci Adv **6** (41), eabb1110.
DOI: 10.1126/sciadv.abb1110